Thermophysics of alkali and related azides II. Heat capacities of potassium, rubidium, cesium, and thallium azides from 5 to 350 K [a,b]

ROBERT W. CARLING [c,d] and EDGAR F. WESTRUM, JR.[e]

Department of Chemistry, University of Michigan, Ann Arbor, Michigan 48109, U.S.A.

The heat capacities of potassium, rubidium, cesium, and thallium azides were determined from 5 to 350 K by adiabatic calorimetry. Although the alkali-metal azides studied in this work exhibited no thermal anomalies over the temperature range studied, thallium azide has a bifurcated anomaly with two maxima at (233.0 ± 0.1) K and (242.04 ± 0.02) K. The associated excess entropy was 0.90 cal_{th} K^{-1} mol^{-1}. The thermal properties of the azides and the corresponding structurally similar hydrogen difluorides are nearly identical. Both have linear symmetrical anions. However, thallium azide shows a solid-solid phase transition not exhibited by thallium hydrogen difluoride. At 298.15 K the values of C_p°, S°, and $-\{G^\circ(T) - H^\circ(0)\}/T$, respectively, are 18.38, 24.86, and 12.676 cal_{th} K^{-1} mol^{-1} for potassium azide; 19.09, 28.78, and 15.58 cal_{th} K^{-1} mol^{-1} for rubidium azide; 19.89, 32.11, and 18.17 cal_{th} K^{-1} mol^{-1} for cesium azide; and 19.26, 32.09, and 18.69 cal_{th} K^{-1} mol^{-1} for thallium azide. Heat capacities at constant volume for KN_3 were deduced from infrared and Raman data.

1. Introduction

An interesting precedent to the study[1] of alkali-metal and thallium azides is the long-standing interest in this laboratory in the orientational disorder of hydrogen difluoride anion, HF_2^- in crystals.[2,3] The isostructural compounds with linear anions — KN_3, RbN_3, CsN_3, and TlN_3—crystallize in distorted CsCl-like structures as do the corresponding hydrogen difluorides. The distortion can be visualized by substituting an azide ion for a chloride ion in CsCl thereby expanding the structure in directions normal to the c-axis. Thus, a tetragonal unit cell is formed with space group, I4/mcm–D_{4h}^{18}.[4]

At elevated temperatures, the tetragonal structure of the alkali-metal azides studied in this research can be expected to transform to a cubic CsCl-like structure due to

thermal disorder of the azide ions. Evidence of cubic high-temperature phases of CsN_3 and RbN_3 occurring at 424 and 588 K, respectively, has been noted.[5] The transition temperature increases with decreasing cation radius and hence the corresponding transition for KN_3 would be expected to occur at approximately 748 K, well above the melting temperature of KN_3. The high-temperature behavior of the alkali-metal azides is supported by the fact that similar behavior is found in the corresponding alkali-metal hydrogen difluorides.[6] The highly ionic azides are relatively stable but do decompose, albeit not violently, at their melting temperatures. As the bonding becomes more covalent the azides become highly explosive and can be detonated by heat, light, shock, and radiation.[7]

Pistorius[8] recently suggested—on the basis of extrapolations of $T(p)$ equilibrium lines assuming negligible curvature—that RbN_3 and CsN_3 at low pressure transform to low-temperature phases near 73 and 143 K, respectively. This would be in contrast to the behavior of the corresponding alkali-metal hydrogen difluorides.[9]

TlN_3 is known to transform—analogously to RbN_3 and CsN_3—to a high-temperature cubic modification. Kezer and Rosenwasser[10] studied this transformation by d.t.a. and reported a transition temperature of 564 K. The reports of low-temperature transitions in TlN_3 are numerous.[4, 8, 11–14] The lowest-temperature phase of TlN_3 is reported to be orthorhombic;[12] a corresponding phase is not found in $TlHF_2$.[9]

Low-temperature adiabatic calorimetry permitted determination of the heat capacities of these azides, the energetics of the transition in TlN_3, and also whether RbN_3 and CsN_3 undergo the low-temperature phase changes predicted by Pistorius.[8]

2. Experimental

SAMPLE PREPARATION AND CHARACTERIZATION

KN_3, RbN_3, and CsN_3. The preparation of each of these azides closely resembles the preparation of the same substances by Suhrmann and Clusius.[15] Optical-grade potassium, rubidium, and cesium carbonates were purchased from Electronic Space Products, Inc., Los Angeles, CA. In a Teflon receiving beaker, 50 g of the desired alkali metal carbonate were dissolved in about 300 cm^3 of water. Excess NaN_3, in the form of an aqueous slush, was put in a round-bottom flask to which a spray trap and condenser were fused. The flask was gently warmed to insure complete dissolution of the NaN_3. To the solution, dilute sulfuric acid (about 12 per cent by mass) was added dropwise from a separatory funnel. The hydrogen azide thus formed distilled into the Teflon receiving beaker, liberated CO_2, and formed the desired alkali-metal azide. The distillation process was continued about 2 h to ensure complete removal of carbon dioxide from the carbonate solution. This procedure was repeated until an adequate amount of each azide was prepared.

Recrystallization of each azide from an aqueous solution was achieved by dissolving the respective azide in water, filtering the solution to remove any insoluble impurities, and then gently heating it until incipient precipitation occurred. After cooling the solution to 300 K, we added a two-fold excess of pure ethanol to enhance precipitation. The precipitated azide was filtered, washed with ethanol, and dried for several hours at 380 K. Each azide was recrystallized three times. RbN_3 was heated only in the

drying oven and was later found to contain trapped solvent. Further details of this determination are postponed until after the presentation of calorimetric results. However, after 2 h in the drying oven, CsN_3 and KN_3 were crushed to uniform size in an agate mortar and placed in a vacuum desiccator over P_2O_5. The dessicator was evacuated for about 4 h through a liquid-nitrogen trap. The samples of CsN_3 and KN_3 were then removed from the desiccator, placed back in the drying oven for about 4 h, and subsequently stored in a desiccator over P_2O_5.

X-ray diffraction analyses of KN_3, RbN_3, and CsN_3 yielded lattice parameters which agree well with those of previous investigations. A comparison of the lattice parameters of these and other azides have been reported previously[16] and is available in a supplementary document.[17]

The azide content of RbN_3 was measured by hydrogen-ion titration after oxidation of the azide ion by nitrite.[18] Although a reasonably good result was obtained by this method (mass per cent azide indicated 39.90±0.05; theoretical: 39.96), this method was abandoned and a more straightforward analysis was undertaken for the azide content of potassium and cesium azides. The azide content was determined gravimetrically by weighing silver azide. Samples of each azide were placed in a beaker and dissolved in 75 cm³ of 8 per cent by mass potassium nitrate solution. Silver nitrate (0.35 mol dm⁻³) was added dropwise to each sample until complete precipitation occurred; the beakers were then stored overnight in the dark. Subsequently the precipitates were filtered in subdued light, rinsed with water, and dried to constant mass in the oven at 380 K. The elemental analysis indicated (51.82±0.02) mass per cent N_3 for KN_3 and (24.03±0.02) mass per cent N_3 for CsN_3 (theoretical: 51.80 and 24.02, respectively).

TlN_3. High-purity thallium was purchased in the form of rods from American Smelting and Refining Company, Central Research Laboratories, South Plainfield, New Jersey. To prepare thallium turnings, the 6 mm diameter rods were first rinsed in concentrated nitric acid to remove any oxide layer present. The turnings generated by "sharpening the rods" in a pencil sharpener were collected in a shallow Teflon dish containing pure ethanol. The turnings were transferred to a Teflon thimble in a Soxhlet apparatus, where they were held in refluxing ethanol for several hours until most of the thallium had reacted. To the ethanol solution a volume of water equal to that of the ethanol was added. The yellow thallium hydroxide precipitate that formed upon addition of the water was filtered and dissolved in warm water. Carbon dioxide, purchased from Matheson and labelled "bone dry", was then bubbled into the thallium hydroxide solution whereupon a white flocculent Tl_2CO_3 precipitate formed. This precipitate was filtered, washed with cold water, and then dried at 380 K for several hours.

Before precipitation of TlN_3, both Tl_2CO_3 and NaN_3 were recrystallized from water. Each solid was dissolved in water and the two solutions were combined whereupon a yellow precipitate of thallium azide immediately formed. The precipitate was filtered, washed with distilled water and pure ethanol, and then dried at 380 K.

The TlN_3 thus prepared was to be recrystallized from water (in which it is not very soluble)[19] so solvent was continually added while heating until total dissolution occurred. The solution was then filtered while still hot to remove insoluble impurities

and allowed to cool slowly to 300 K while long acicular yellow crystals formed. These crystals were filtered, washed with pure ethanol and then dried for 6 h at 380 K. The recrystallization process was repeated three times and the product stored in a desiccator over $CaSO_4$.

X-ray diffraction analysis of TlN_3 yielded lattice parameters which are in excellent accord with those of other investigators.[16, 17] The thallium content was determined by a volumetric titration with standard potassium iodate solution as the titrant.[20] The azide solution required gentle warming completely to dissolve the TlN_3 before analysis. Elemental analysis indicated (82.92 ± 0.02) mass per cent Tl (theoretical: 82.94). Further analyses of the sample were performed after the heat-capacity determinations were completed and will be discussed later.

Loading details. Heat-capacity measurements for all four samples were made in the Mark II adiabatic cryostat.[1, 21] Loading information for these samples is given in table 1.

TABLE 1. Calorimeter loading information

Compound	Calorimeter no.	V cm^3	M [a] $g\,mol^{-1}$	m g	$p(He)$ kPa	ρ [b] $g\,cm^{-3}$
KN_3	W–52	59.11	81.118	50.2650	6.6	2.032
RbN_3	W–28	92.31	127.487	84.8699 [c]	5.7	2.825
CsN_3	W–52	59.11	174.922	46.1975	7.6	3.384
TlN_3	W–52	59.11	246.3901	89.3849 [c]	6.5	5.769

[a] Based on 1968 IUPAC scale of atomic weights.
[b] Crystallographic density from lattice parameters of this research, four molecules per unit cell.
[c] Mass corrected for traces of water present.

3. Results

HEAT CAPACITY VALUES FOR KN_3, RbN_3, AND CsN_3

Heat capacities in chronological sequence at the mean temperatures of determination are presented in tables 2 and 3. Approximate temperature increments can usually be inferred from adjacent mean temperatures. These results have been adjusted for curvature and are considered to have a probable error of about 5 per cent at 5 K, decreasing to 1 per cent at 10 K, and to less than 0.1 per cent above 20 K. The values are based upon IPTS—48. Results from several series of determinations taken to ascertain the enthalpy increment through the bifurcated anomaly in TlN_3 have been summarized in table 4.

Molar heat-capacity curves for KN_3, RbN_3, and CsN_3 are displayed in figure 1. No thermal anomalies due to structural changes in these compounds were observed; however, the heat capacity of RbN_3 revealed a small bump located at (257.3 ± 0.8) K which was believed to result from the fusion of water trapped in the sample. To test this interpretation, the freezing temperature of a saturated RbN_3 aqueous solution was determined with a Hewlett-Packard quartz thermometer as 257.5 K and supports the interpretation of the anomaly as due to residual water trapped in the RbN_3

TABLE 2. Heat capacities of KN_3, RbN_3, and CsN_3

$(cal_{th} = 4.184\ J)$

T / K	C_p / cal_{th} K⁻¹ mol⁻¹	T / K	C_p / cal_{th} K⁻¹ mol⁻¹	T / K	C_p / cal_{th} K⁻¹ mol⁻¹	T / K	C_p / cal_{th} K⁻¹ mol⁻¹
				KN₃			
	Series I	347.39	19.43		Series III	23.99	1.012
						26.31	1.329
209.54	16.16		Series II	5.64	0.014	28.73	1.688
215.15	16.34			7.07	0.023	31.44	2.137
223.78	16.56	96.01	11.26	8.28	0.036	34.76	2.727
233.99	16.83	103.34	11.80	9.38	0.053	38.69	3.456
244.27	17.08	112.49	12.39	10.34	0.074	43.12	4.281
254.43	17.34	121.94	12.93	11.39	0.089	48.08	5.194
264.66	17.59	131.74	13.44	12.62	0.120	53.44	6.140
275.45	17.84	141.94	13.90	12.52	0.119	58.85	7.025
286.31	18.10	152.25	14.31	13.96	0.173	64.69	7.914
296.79	18.34	162.66	14.71	15.29	0.238	70.70	8.707
307.45	18.57	173.04	15.09	16.73	0.317	76.23	9.373
318.30	18.81	183.20	15.40	18.35	0.434	81.99	10.02
329.04	19.04	193.42	15.69	20.06	0.583	89.11	10.72
339.68	19.26	203.69	16.00	21.90	0.768	97.59	11.39
		213.79	16.29				
				RbN₃			
	Series I	56.54	8.558	7.44	0.072	261.90	18.90
		63.72	9.599	8.14	0.086		
149.25	15.13	71.17	10.48	8.92	0.123		Series VI
151.62	15.23	77.96	11.19	9.72	0.171		
157.68	15.45	84.28	11.80	10.56	0.234	242.74	17.78
166.99	15.75	91.21	12.34	11.48	0.270	ΔH Detn.	
176.96	16.05	98.77	12.82	12.98	0.424	280.69	18.85
187.02	16.34	107.01	13.30	13.96	0.545		
196.92	16.60	115.94	13.76	14.95	0.678		Series VII
206.88	16.87			16.17	0.840		
216.91	17.14		Series III	17.59	1.061	243.18	17.78
226.81	17.39			19.14	1.318	ΔH Detn.	
236.78	17.65	103.92	13.12	20.93	1.644	268.04	18.44
246.82	17.92	113.12	13.63	23.05	2.043		
256.72		121.95	14.06	25.62	2.566		Series VIII
266.60	18.44	131.35	14.47	28.52	3.165		
277.09	18.67	141.32	14.87	31.64	3.831	242.84	17.77
287.47	18.92	151.03	15.22	35.12	4.584	247.56	17.94
297.75	19.18	160.52	15.53	38.74	5.337	251.31	18.16
308.25	19.42			44.07	6.399	253.64	18.29
318.98	19.67		Series IV	48.30	7.219	255.50	18.46
329.60	19.90			53.17	8.025	257.28	20.08
340.14	20.14	4.18	0.000	58.82	8.900	259.03	19.29
346.18	20.22	4.74	0.020			260.84	18.66
		5.27	0.020		Series V	262.69	18.46
	Series II	5.76	0.028			265.00	18.39
		6.26	0.037	242.81	17.82	268.69	18.49
51.78	7.794	6.80	0.047	252.44	18.46		

TABLE 2—continued

$\dfrac{T}{K}$	$\dfrac{C_p}{cal_{th}\ K^{-1}\ mol^{-1}}$	$\dfrac{T}{K}$	$\dfrac{C_p}{cal_{th}\ K^{-1}\ mol^{-1}}$	$\dfrac{T}{K}$	$\dfrac{C_p}{cal_{th}\ K^{-1}\ mol^{-1}}$	$\dfrac{T}{K}$	$\dfrac{C_p}{cal_{th}\ K^{-1}\ mol^{-1}}$
					CsN₃		
	Series I		Series II	204.93	17.29	16.27	1.808
				214.23	17.54	17.96	2.192
215.77	17.60	66.07	11.06			19.82	2.615
226.49	17.90	74.63	11.88		Series III	21.88	3.079
236.66	18.16	82.73	12.59			23.91	3.540
247.37	18.44	91.14	13.20	4.56	0.020	26.00	4.022
257.96	18.73	100.42	13.70	4.94	0.062	28.64	4.620
268.42	19.01	110.50	14.18	5.36	0.076	32.02	5.381
278.78	19.31	120.90	14.62	6.40	0.137	36.10	6.267
289.00	19.62	131.20	15.02	7.32	0.207	40.50	7.165
299.11	19.92	141.80	15.40	8.25	0.309	45.01	8.010
309.67	20.23	152.73	15.76	9.25	0.456	49.64	8.841
320.30	20.53	163.40	16.09	10.41	0.646	54.66	9.579
330.48	20.83	173.85	16.41	11.75	0.857	59.78	10.29
340.55	21.14	184.11	16.70	13.26	1.162	65.20	10.96
347.55	21.36	194.46	17.00	14.75	1.490	71.76	11.63

TABLE 3. Heat capacity of TlN₃

$(cal_{th} = 4.184\ J)$

$\dfrac{T}{K}$	$\dfrac{C_p}{cal_{th}\ K^{-1}\ mol^{-1}}$	$\dfrac{T}{K}$	$\dfrac{C_p}{cal_{th}\ K^{-1}\ mol^{-1}}$	$\dfrac{T}{K}$	$\dfrac{C_p}{cal_{th}\ K^{-1}\ mol^{-1}}$	$\dfrac{T}{K}$	$\dfrac{C_p}{cal_{th}\ K^{-1}\ mol^{-1}}$
	Series I		ΔH Detn A	4.54	0.052	47.91	8.609
				4.96	0.071	52.80	9.326
		265.15	18.52	5.38	0.139	53.40	10.08
91.52	13.11	275.68	21.04	6.06	0.178	64.11	10.78
99.80	13.56	285.88	18.95	6.64	0.222	70.07	11.37
109.92	14.06	296.42	19.18	7.28	0.318	76.92	11.99
120.47	14.54	306.85	19.44	8.02	0.440	84.72	12.64
130.62	14.96	317.17	19.70	8.79	0.601	93.42	13.19
141.02	15.35	327.40	19.95	9.62	0.815	102.93	13.69
151.68	15.72	337.53	20.22	10.66	1.057		
162.09	16.05	346.14	20.44	11.95	1.315		Series VII
172.29	16.37			13.41	1.679		
182.30	16.66		Series III	15.01	2.082	226.74	17.96
192.71	16.96			16.72	2.493		ΔH Detn B
203.51	17.26		(see below)	18.53	2.912	260.36	18.39
214.15	17.61			20.40	3.338		ΔH Detn C
224.63	17.90		Series IV	22.29	3.757	286.86	18.93
232.84	38.06			24.25	4.186		
239.78	26.75		(see below)	26.43	4.637		Series VIII
248.77	18.53			28.94	5.158		
258.90	18.36		Series V	32.10	5.760		(See below)
				35.68	6.503		
	Series II		(see below)	39.63	7.219		Series IX
				43.66	7.919		
220.70	17.76		Series VI				(see below)

TABLE 3—continued

$\dfrac{T}{K}$	$\dfrac{\Delta T}{K}$	$\dfrac{\langle C_p \rangle}{cal_{th}\,K^{-1}\,mol^{-1}}$ [a]	$\dfrac{C_p}{cal_{th}\,K^{-1}\,mol^{-1}}$ [b]	$\dfrac{T}{K}$	$\dfrac{\Delta T}{K}$	$\dfrac{\langle C_p \rangle}{cal_{th}\,K^{-1}\,mol^{-1}}$ [a]	$\dfrac{C_p}{cal_{th}\,K^{-1}\,mol^{-1}}$ [b]
		Series III		274.37	0.91	19.00	18.85
				275.27	0.92	18.91	18.78
228.77	4.20	18.10	18.04	276.84	2.28	18.69	18.76
231.90	2.06	28.66	18.57				
233.24	0.70	104.3	100.6			**Series V**	
234.34	1.54	41.81	41.81				
236.18	2.17	26.68	26.57	227.62	4.71	18.02	18.02
238.43	2.38	23.39	23.33	ΔH Detn E			
240.74	2.26	25.20	24.53	ΔH Detn F			
242.83	1.94	31.00	30.75	270.30	1.98	19.28	19.28
245.16	2.77	18.58	18.68	271.72	0.90	21.17	21.10
247.94	2.79	18.37	18.37	272.48	0.67	32.27	26.90
251.42	4.19	18.30	18.30	273.16	0.76	27.35	20.06
				274.01	0.97	19.00	18.94
		Series IV		275.52	2.10	19.06	18.77
				277.62	2.12	18.73	18.73
228.22	3.55	18.03	18.03				
230.25	0.52	18.12	18.12			**Series VIII**	
230.77	0.52	18.22	18.20				
231.28	0.52	18.25	18.34	240.45	2.03	24.17	23.96
231.80	0.52	18.52	18.52	241.61	0.31	27.20	27.20
232.31	0.51	18.82	18.86	241.83	0.13	35.28	35.28
232.73	0.34	33.09	19.71	241.94	0.09	55.34	55.34
233.00	0.30	123.2	123.2	242.00	0.04	118.6	118.6
233.27	0.35	95.66	95.66	242.04	0.03	164.1	164.1
233.66	0.50	64.63	64.63	242.08	0.07	76.53	76.53
234.22	0.68	44.52	43.90	271.33	1.82	20.39	20.29
234.96	0.86	33.28	33.28	272.29	0.18	24.58	24.26
235.86	0.98	27.67	27.67	272.41	0.09	26.11	26.11
236.87	1.06	24.94	24.94	272.49	0.08	26.95	27.78
237.93	1.10	23.60	23.60	272.56	0.08	29.90	29.90
239.03	1.12	23.20	23.20	272.62	0.07	32.13	32.13
240.13	1.10	23.62	23.62	272.71	0.13	36.96	36.96
241.19	1.04	25.59	25.59				
241.97	0.53	59.98	72.00			**Series IX**	
242.48	0.50	24.00	24.00				
243.00	0.56	20.35	20.35	231.50	2.63	19.44	18.40
243.94	1.32	19.17	19.17	232.84	0.10	25.61	25.61
245.27	1.35	18.66	18.66	232.90	0.09	30.40	30.40
ΔH Detn D				232.94	0.08	35.44	35.44
273.48	0.90	19.42	19.39	232.98	0.07	38.42	45.00

[a] The symbol $\langle C_p \rangle$ represents mean values of the heat capacity as calculated directly from finite $\Delta H/\Delta T$ without curvature correction.

[b] The symbol C_p in columns adjacent to $\langle C_p \rangle$ represents the value of the heat capacity read from the smoothed curve at temperature T. Elsewhere in the table it represents C_p analytically corrected for curvature.

TABLE 4. Enthalpy determinations for overlapping anomalies in TlN_3

$$(cal_{th} = 4.184\ J)$$

Designation	$\dfrac{T_1}{K}$	$\dfrac{T_2}{K}$	$\dfrac{H°(T_2)-H°(T_1)}{cal_{th}\ mol^{-1}}$	$\dfrac{H°(261\ K)-H°(220\ K)}{cal_{th}\ mol^{-1}}$
A (Series II)	225.91	259.52	804.93	937.63
B (Series V)	229.97	253.80	627.90	938.30
E (Series VII)	229.11	255.54	675.64	938.22
			Mean:	938.0 ± 0.5
			Lattice:	$742._1 \pm 2$
			Excess:	$195._9 \pm 2$
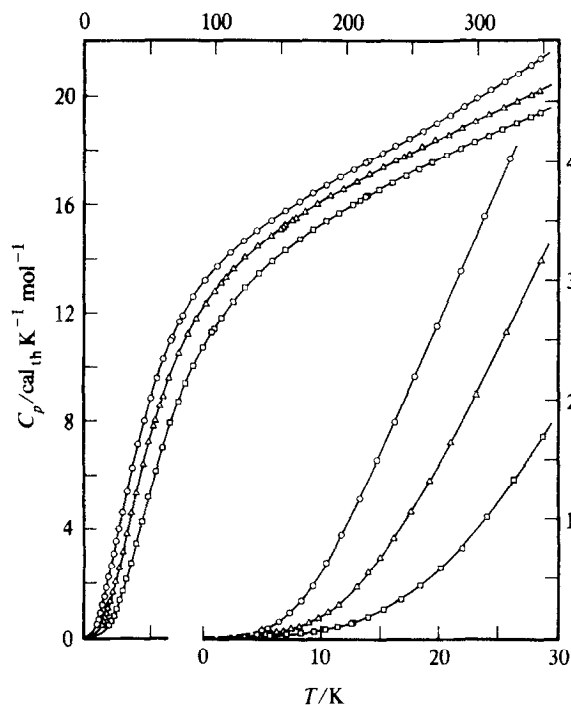
FIGURE 1. Experimental heat capacities: $\square$, KN_3; $\triangle$, RbN_3; $\bigcirc$, CsN_3.

sample. From the excess enthalpy in the region of this small bump divided by the enthalpy of fusion of water,[22] a value 0.07 mass per cent of H_2O was computed.

HEAT CAPACITY VALUES FOR TlN_3

The molar heat capacity of TlN_3 displayed in figures 2 and 3 revealed a bifurcated anomaly with the two maxima occurring at (233.0 ± 0.1) and (242.04 ± 0.02) K. In addition, a small bump at 272.7 K was thought to be due to the fusion of water in the sample. Iqbal and Malhotra[11] noted a transition in the Raman spectra occurring on
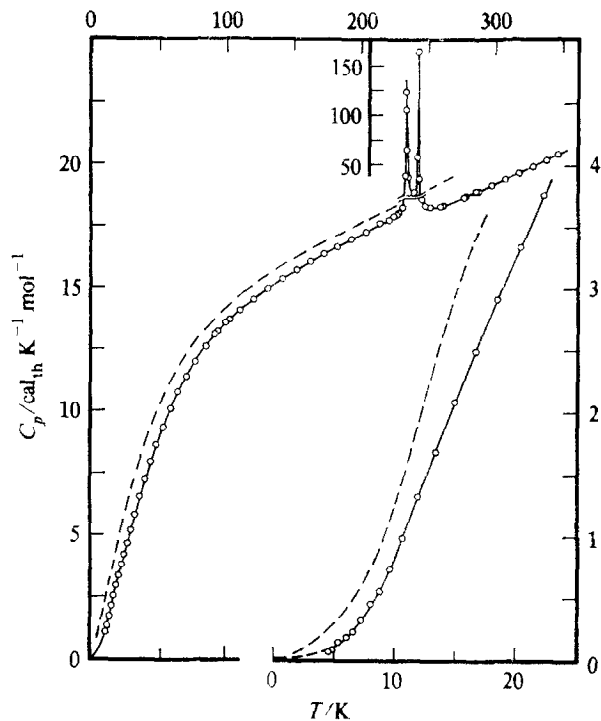
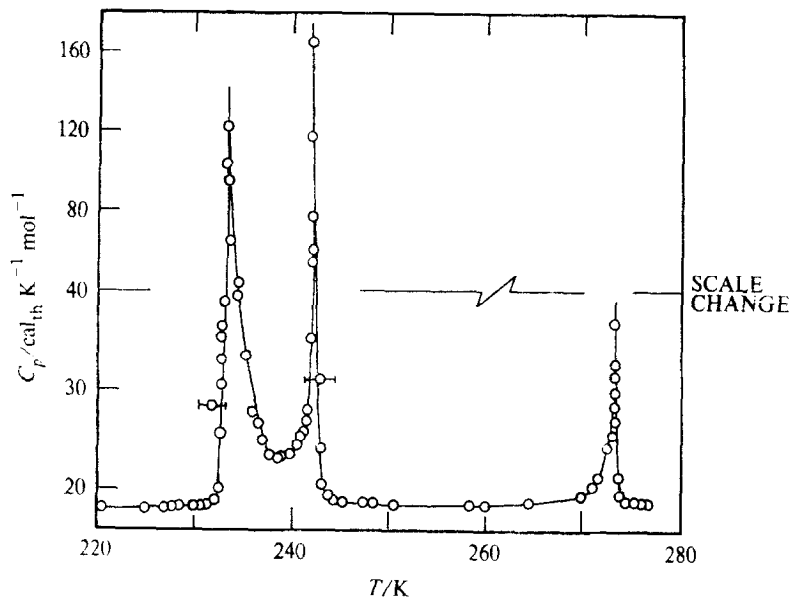FIGURE 2. Experimental heat capacities: ——, TlN₃; – – –, TlHF₂.

FIGURE 3. Experimental heat capacity of TlN₃ in the region of the the two transitions and the thermal anomaly attributed to the presence of water. ○, experimental values; ——, smoothed curve (compare text).

warming to 278 K. On cooling the sample two of the spectral bands split into four bands at 269 K and persisted as low as 95 K. Iqbal now considers that his previous interpretation of a phase change at 278 K is incorrect,[23] and that his spectral result was due to sluggishness of the first-order transition near 240 K when the crystal was warmed slowly. Several analytical tests were performed to ascertain the presence or absence of water in the sample. An infrared spectrum was taken on a Nujol mull, but nothing found could be attributed to water. The freezing temperature of a saturated aqueous TlN_3 solution was determined with a Hewlett-Packard quartz thermometer as only -0.03 K, more than 0.4 K above the observed anomaly. Although the infrared spectrum taken on the calorimetric sample of TlN_3 showed no evidence of water in the sample, the concentration of water may have been below detection limits. Recent neutron-diffraction experiments down to about 250 K show no evidence of a transition near 270 K.[4] The excess enthalpy (about 17.8 cal_{th} mol^{-1}) in the region of this anomaly is, therefore, attributed to water, the mass fraction of which is estimated to be 0.001 based on the enthalpy of fusion of water.[22]

IMPURITY ADJUSTMENT

Adjustments for the small amount of water in the samples of RbN_3 and TlN_3 were made on the experimental heat capacity by the use of the heat capacity of pure water determined by Giauque and Stout.[24] These corrections have been made on all RbN_3 and TlN_3 values in tables 5 and 6, with the exception of the results taken in the vicinity of the fusion maxima.

TABLE 5. Thermophysical properties of KN_3, RbN_3, snd CsN_3
($cal_{th} = 4.184$ J)

$\dfrac{T}{K}$	$\dfrac{C_p}{cal_{th}\ K^{-1}\ mol^{-1}}$	$\dfrac{S^\circ(T)-S^\circ(0)}{cal_{th}\ K^{-1}\ mol^{-1}}$	$\dfrac{H^\circ(T)-H^\circ(0)}{cal_{th}\ mol^{-1}}$	$\dfrac{-\{G^\circ(T)-H^\circ(0)\}/T}{cal_{th}\ K^{-1}\ mol^{-1}}$
		KN_3		
5	0.008	(0.003)	(0.010)	(0.001)
10	0.060	0.022	0.167	0.006
15	0.220	0.071	0.798	0.018
20	0.576	0.178	2.700	0.043
25	1.444	0.364	6.916	0.088
30	1.895	0.637	14.450	0.155
35	2.771	0.994	26.078	0.249
40	3.693	1.424	42.232	0.368
45	4.620	1.912	63.02	0.512
50	5.525	2.446	88.39	0.678
60	7.198	3.605	152.19	1.068
70	8.631	4.825	231.55	1.517
80	9.816	6.058	323.98	2.008
90	10.783	7.272	427.14	2.526
100	11.577	8.450	539.1	3.059
110	12.242	9.586	658.3	3.601
120	12.817	10.676	783.6	4.146
130	13.327	11.722	914.4	4.689
140	13.791	12.727	1050.0	5.227
150	14.218	13.694	1190.1	5.760
160	14.614	14.624	1334.3	6.285
170	14.979	15.52	1482.3	6.802

TABLE 5—*continued*

T K	C_p cal_{th} K^{-1} mol^{-1}	$S°(T) - S°(0)$ cal_{th} K^{-1} mol^{-1}	$H°(T) - H°(0)$ cal_{th} mol^{-1}	$-\{G°(T) - H°(0)\}/T$ cal_{th} K^{-1} mol^{-1}
180	15.32	16.39	1633.7	7.310
190	15.63	17.22	1788.5	7.810
200	15.91	18.03	1946.2	8.301
210	16.19	18.82	2106.7	8.783
220	16.45	19.57	2269.9	9.257
230	16.70	20.31	2435.7	9.721
240	16.96	21.03	2604.0	10.178
250	17.21	21.73	2774.9	10.626
260	17.47	22.41	2948.3	11.066
270	17.72	23.07	3124.2	11.498
280	17.97	23.72	3302.7	11.923
290	18.20	24.35	3483.6	12.341
300	18.42	24.97	3666.7	12.751
310	18.63	25.58	3851.9	13.156
320	18.83	26.18	4039.2	13.553
330	19.04	26.76	4228.6	13.945
340	19.26	27.33	4420.1	14.330
350	19.49	27.89	4613.9	14.709
273.15	17.80	23.28	3180.2	11.633
298.15	18.38	24.86	3632.6	12.676
		RbN₃		
5	0.014	(0.007)	(0.027)	(0.002)
10	0.181	0.055	0.420	0.014
15	0.673	0.210	2.402	0.049
20	1.471	0.507	7.665	0.124
25	2.432	0.936	17.377	0.241
30	3.475	1.471	32.120	0.400
35	4.551	2.088	52.19	0.596
40	5.585	2.764	77.56	0.825
45	6.569	3.479	107.97	1.080
50	7.482	4.219	143.13	1.356
60	9.072	5.728	226.16	1.959
70	10.357	7.227	323.55	2.605
80	11.381	8.679	432.43	3.274
90	12.203	10.069	550.5	3.952
100	12.878	11.391	676.0	4.631
110	13.449	12.646	807.7	5.303
120	13.945	13.837	944.7	5.965
130	14.388	14.972	1086.4	6.614
140	14.788	16.05	1232.3	7.250
150	15.15	17.09	1382.1	7.872
160	15.49	18.07	1535.3	8.479
170	15.81	19.02	1691.8	9.071
180	16.10	19.94	1851.4	9.650
190	16.38	20.81	2013.8	10.214
200	16.65	21.66	2179.0	10.765
210	16.92	22.48	2346.9	11.304
220	17.19	23.27	2517.4	11.830
230	17.45	24.04	2690.6	12.344
240	17.71	24.79	2866.4	12.847
250	17.96	25.52	3044.8	13.340
260	18.21	26.23	3225.6	13.822
270	18.45	26.92	3408.9	14.294

TABLE 5—continued

$\dfrac{T}{K}$	$\dfrac{C_p}{cal_{th}\,K^{-1}\,mol^{-1}}$	$\dfrac{S°(T)-S°(0)}{cal_{th}\,K^{-1}\,mol^{-1}}$	$\dfrac{H°(T)-H°(0)}{cal_{th}\,mol^{-1}}$	$\dfrac{-\{G°(T)-H°(0)\}/T}{cal_{th}\,K^{-1}\,mol^{-1}}$
280	18.68	27.59	3594.5	14.757
290	18.91	28.25	3782.5	15.21
300	19.14	28.90	3972.7	15.66
310	19.37	29.53	4165.2	16.09
320	19.59	30.15	4360.0	16.52
330	19.82	30.76	4557.1	16.95
340	20.04	31.35	4756.4	17.36
350	20.25	31.93	4957.9	17.77
273.15	18.52	27.13	3467.1	14.441
298.15	19.09	28.78	3937.4	15.58
		CsN$_3$		
5	0.051	(0.001)	(0.003)	(0.000)
10	0.564	0.161	1.303	0.031
15	1.533	0.563	6.420	0.135
20	2.656	1.157	16.874	0.313
25	3.789	1.871	32.987	0.552
30	4.926	2.662	54.77	0.837
35	6.038	3.506	82.21	1.157
40	7.062	4.380	115.00	1.505
45	8.002	5.267	152.69	1.874
50	8.858	6.155	194.88	2.258
60	10.319	7.904	291.03	3.054
70	11.477	9.585	400.24	3.868
80	12.386	11.180	519.7	4.683
90	13.102	12.681	647.3	5.489
100	13.679	14.093	781.3	6.280
110	14.161	15.42	920.6	7.051
120	14.581	16.67	1064.3	7.801
130	14.964	17.85	1212.1	8.529
140	15.32	18.97	1363.5	9.235
150	15.66	20.04	1518.4	9.921
160	15.99	21.06	1676.7	10.585
170	16.30	22.04	1838.2	11.231
180	16.60	22.98	2002.7	11.858
190	16.89	23.89	2170.1	12.467
200	17.17	24.76	2340.4	13.060
210	17.44	25.61	2513.4	13.638
220	17.70	26.42	2689.1	14.201
230	17.97	27.22	2867.4	14.749
240	18.24	27.99	3048.4	15.28
250	18.51	28.74	3232.2	15.81
260	18.79	29.47	3418.6	16.32
270	19.07	30.18	3608.0	16.82
280	19.36	30.88	3800.1	17.31
290	19.65	31.57	3995.2	17.79
300	19.94	32.24	4193.2	18.26
310	20.23	32.90	4394.0	18.72
320	20.52	33.54	4597.8	19.17
330	20.82	34.18	4804.5	19.62
340	21.12	34.80	5014	20.06
350	21.43	35.42	5227	20.49
273.15	19.16	30.40	3668.2	16.98
298.15	19.89	32.11	4156.3	18.17

TABLE 6. Thermophysical properties of TIN_3
$(cal_{th} = 4.184\ J)$

$\dfrac{T}{K}$	$\dfrac{C_p}{cal_{th}\ K^{-1}\ mol^{-1}}$	$\dfrac{S°(T)-S°(0)}{cal_{th}\ K^{-1}\ mol^{-1}}$	$\dfrac{H°(T)-H°(0)}{cal_{th}\ mol^{-1}}$	$\dfrac{-\{G°(T)-H°(0)\}/T}{cal_{th}\ K^{-1}\ mol^{-1}}$
5	0.076	(0.033)	(0.125)	(0.008)
10	0.874	0.277	2.117	0.066
15	2.073	0.856	9.457	0.226
20	3.247	1.615	22.791	0.476
25	4.333	2.458	41.779	0.787
30	5.356	3.339	66.02	1.139
35	6.350	4.240	95.30	1.517
40	7.283	5.150	129.42	1.914
45	8.122	6.057	167.96	2.324
50	8.890	6.953	210.54	2.743
60	10.206	8.694	306.23	3.591
70	11.295	10.352	413.91	4.439
80	12.195	11.921	531.5	5.277
90	12.941	13.402	657.3	6.098
100	13.561	14.798	789.9	6.899
110	14.084	16.12	928.2	7.678
120	14.530	17.36	1071.3	8.433
130	14.919	18.54	1218.6	9.166
140	15.27	19.66	1369.6	9.876
150	15.59	20.72	1523.9	10.564
160	15.89	21.74	1681.3	11.231
170	16.19	22.71	1841.7	11.878
180	16.49	23.64	2005.1	12.505
190	16.78	24.54	2171.4	13.116
200	17.08	25.41	2340.8	13.709
210	17.39	26.25	2513.1	14.286
220	17.70	27.07	2688.6	14.849
230	18.02	27.86	2867.2	15.40
233.00 [a]	123.2			
242.04 [a]	164.1			
250	18.11	29.90	3068.7	17.62
260	18.40	30.62	3251.3	18.11
270	18.63	31.32	3436.5	18.59
280	18.85	32.00	3623.9	19.05
290	19.07	32.66	3813.5	19.51
300	19.30	33.31	4005.3	19.96
310	19.54	33.95	4199.5	20.40
320	19.80	34.57	4396.2	20.84
330	20.06	35.19	4595.4	21.26
340	20.32	35.79	4797.3	21.68
350	20.57	36.38	5001.7	22.09
273.15	18.70	31.53	3495.3	18.74
298.15	19.25	33.19	3969.6	19.88

[a] Peak of transition

69

THERMAL FUNCTIONS

The experimental heat capacities in the non-transition regions were curve-fitted to polynomials in reduced temperature by the method of least-squares and then integrated to yield values of the thermal functions at regular temperature intervals presented in tables 5 and 6. The thermodynamic functions have a probable error of less than 0.1 per cent above 50 K. Below 5 K, entropy and enthalpy increments were obtained from plots of C_p/T against T^2. No adjustments for contributions due to isotopic mixing or nuclear spin were made; hence, the values tabulated are practical values for use in chemical thermodynamic calculations.

4. Discussion

POTASSIUM, RUBIDIUM, AND CESIUM AZIDES

That KN_3, RbN_3, and CsN_3 have no low-temperature thermal anomalies in the heat capacity is shown in figure 1. Pistorius predicted low-temperature phase transitions for RbN_3 and CsN_3[8] based on the assumption that $p(T)$ equilibrium lines could be extrapolated linearly to 101 kPa. These lines may be concave downwards so that the low-temperature phases of RbN_3 and CsN_3 would only be encountered at higher pressures. A similar prediction by White and Pistorius[25] was made for $CsHF_2$, but no thermal anomaly was detected below 300 K in heat-capacity measurements of $CsHF_2$.[2] For $CsHF_2$, as for RbN_3 and CsN_3, this phase transition would only be encountered at pressures higher than 100 kPa. An extrapolation similar to that for $CsHF_2$ is not possible for $RbHF_2$ because the phase diagram is incomplete.

Figure 4 illustrates the heat capacities of KN_3, RbN_3, and CsN_3 and those of the respective MHF_2's to facilitate comparison between the azides and the hydrogen difluorides. The similarities are to be expected since all the compounds consist of linear, symmetrical anions which belong to the same space group, I4/mcm-D_{4h}^{18}, and the contributions from internal frequencies of the anions are small. The only difference arises from the slightly larger molar masses of the azides relative to their respective hydrogen difluorides. Table 7 cites the entropies at 298.15 K for the azides and the corresponding hydrogen difluorides for further comparison.

THALLIUM AZIDE

Reproducibility of enthalpy increments over the transition region is shown in table 4. The lattice heat capacity was deduced from graphical extrapolations of effective Θ_D's against temperature into the transition region from above and below to get two values of Θ_D(lattice). These values of Θ_D(lattice) between 220 and 261 K were converted to lattice heat-capacity values extrapolated to 242 K to evaluate the excess enthalpy and entropy. From the difference between the integrated experimental heat-capacity curve and the estimated lattice contribution the total enthalpy and entropy of the transitions were obtained. The lattice enthalpy $\{H°(261\ K) - H°(220\ K)\}$ was determined to be 742.1 cal_{th} mol^{-1}. The resulting entropy and enthalpy increments of the transitions were found to be $\Delta S_t = (0.89 \pm 0.01)\ cal_{th}\ K^{-1}\ mol^{-1}$ and $\Delta H_t = (195._9 \pm 2)$ $cal_{th}\ mol^{-1}$. If a lower estimate of the lattice contribution had been chosen the lattice enthalpy $\{H°(261\ K) - H°(220\ K)\}$ would have been 738 $cal_{th}\ mol^{-1}$. The
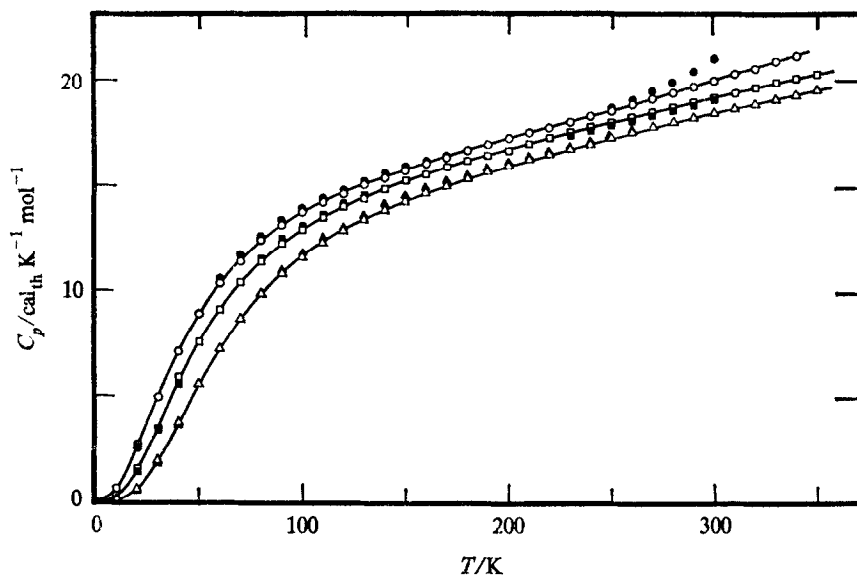
FIGURE 4. Smoothed heat capacities. △, KN_3; ▲, KHF_3; □, RbN_2; ■, $RbHF_2$; ○, CsN_3; ●, $CsHF_2$. Data for the MHF_2 compounds are from Burney and Westrum.[9]

TABLE 7. Entropies for the azides and hydrogen difluorides at 298.15 K
(cal_{th} = 4.184 J)

Cation	Na	K	Rb	Cs	Tl
$S(MN_3)/cal_{th}$ K^{-1} mol^{-1}	23.15 [a]	24.86	28.78	32.11	33.19
$S(MHF_2)/cal_{th}$ K^{-1} mol^{-1}	21.73 [b]	24.92 [c]	28.70 [d]	32.30 [d]	34.92 [d]

[a] Carling and Westrum.[1] [b] Burney and Westrum.[2] [c] Westrum and Pitzer.[3] [d] Burney and Westrum.[9]

resulting total entropy and enthalpy increments of the transitions would have been $\Delta S_t = (0.91 \pm 0.01)$ cal_{th} K^{-1} mol^{-1} and $\Delta H_t = (200._5 \pm 2)$ cal_{th} mol^{-1}. Although the thermal properties of the components of the bifurcated anomaly cannot be resolved unambiguously, the apparent enthalpies and entropies associated with the lower peak are chosen as (160 ± 10) cal_{th} mol^{-1} and (0.71 ± 0.05) cal_{th} K^{-1} mol^{-1} and with the upper (40 ± 10) cal_{th} mol^{-1} and (0.18 ± 0.05) cal_{th} K^{-1} mol^{-1}, respectively.

Thermal effects in TlN_3 have been studied by a variety of other methods also. A phase transition detected by d.t.a. at about 233 K has been reported.[3] The infrared and Raman spectra indicated transition temperatures of 225 K,[11,26] and 240 K.[13] A readily reversible transition at (248 ± 5) K was found in the thermal expansion.[12] Pressure equilibrium studies indicated a transition at (193 ± 30) K.[8] More recent d.t.a. work[14] indicated a transition temperature of (243.4 ± 1.0) K. Although evidence for two closely-spaced transitions has not previously been reported, it seems plausible that the range in reported transition temperatures observed by different techniques may arise from one or other of the two transitions observed in the present research.

The present work has yielded two transitions at 233 and 242 K and the following discussion is an attempt to elucidate the phase relations at high pressures for TlN_3. Figure 5a shows the phase diagram based on the work of Pistorius.[14] Recent attempts to resolve the problems in the light of the present results using d.t.a. at high pressures[27] produced no additional information. A lack of reproducibility and the minute size of d.t.a. signals involved do not allow definite conclusions. Calorimetric studies under hydrostatic pressure conditions or high-pressure X-ray diffraction studies would be most useful in resolving the situation.

The first possibility is that the two transitions present merge at higher pressures at a IV/III/II triple point, and the resulting phase boundary is the III/II boundary reported by Pistorius. Close examination of the determined slope of the III/II phase boundary shows this to be impossible. An added disqualification is the fact that the high volume change present at the III/II transition was not apparent in the transition from the II to IV phase. (Pistorius presents a detailed discussion of this.)[14]
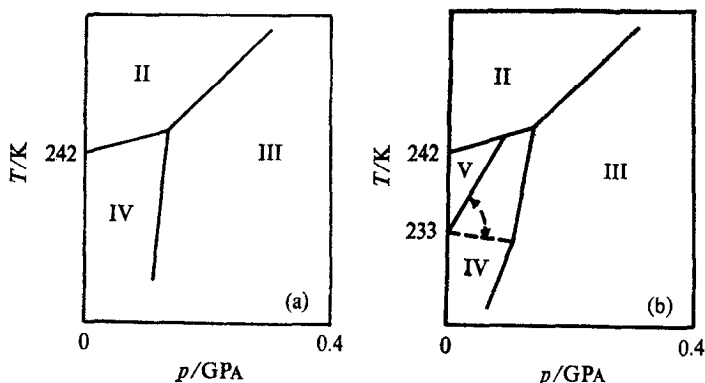
FIGURE 5. (a) Phase diagram at low pressures of TlN_3 system according to Pistorius;[14] (b) possible revision proposed by Clark.[27]

There remain two possibilities which are both acceptable. Figure 5b illustrates two possible slopes for a proposed IV/V phase boundary. The first one indicates a II/V/IV triple point at 0.15 GPa near 244 K. This value is chosen because of the disappearance of d.t.a. signals reported by Pistorius at this point. From this assumption it is possible to calculate the volume changes on the IV/V and V/II boundaries using the Clausius–Clapeyron equation. These support the contention that the IV/III phase boundary carries most of the volume change associated with the III/II transition. The unique feature shown in figure 5b is the existence of phase IV which is different from phase III. The existence of this phase has an added importance because it alters certain crystal-chemical arguments concerning the high-pressure phases $TlN_3(III)$, $RbN_3(III)$, and $CsN_3(III)$. From previous data on all compounds mentioned, arguments have been advanced[14] to show that these phases are probably isostructural and that they are related to the orthorhombic low-temperature phase[12,28] found for TlN_3 at atmospheric pressure. However, Raman data[29] are said to provide evidence that

these phases may, in fact, be different. The presence of the TlN$_3$ IV/III phase boundary indicates that they are apparently so. The change from the tetragonal phase II through phase IV, and finally to phase III may be from an eight-fold to a 4–4 coordination with four long azide—metal bonds and four short azide – metal bonds.[12] Such 4 – 4 coordination has been observed in AgN$_3$,[29] with distortion which is a consequence of weak covalent bonding between the azide and the thallium ions. At higher temperature the thermal energy masks these distortions.

Since "aged" samples of TlN$_3$ are reported to exhibit a transition at 225 K,[13] we note that the calorimetric sample employed in our endeavor was about six months old. Until details of this "time-dependent" transition are known ,we consider the reported transition at 225 K to be that observed at 233 K in this study.

As in the comparison between NaN$_3$ and NaHF$_2$,[1] it is noted that TlN$_3$ and TlHF$_2$ do not exhibit the same thermal behavior; the entropy at 298.15 K of TlHF$_2$ is about 5 per cent larger than that of TlN$_3$ (compare table 7). Hassel *et al.*[31] performed analytical tests and an X-ray diffraction analysis on a material initially identified as TlHF$_2$. These analytical tests were later shown to be incorrect and the proper formula of the compound identified as TlH$_2$F$_3$.$\frac{1}{2}$H$_2$O.[32] Lee[33] suggested that the heat-capacity determinations by Burney[9] might have been taken on a sample of the hemihydrate. If the calorimetric TlHF$_2$ sample, whose heat capacity and composition were determined in this laboratory, was partially hydrated this might explain the seemingly large value of $S°$ for thallium hydrogen difluoride at 298.15 K. However, the analysis of the calorimetric sample of TlHF$_2$ was in good agreement with theoretical.[9] Evidence for hydration such as Hassel encountered was sought but not detected.

It seems probable that the difference in $S°$(298.15 K) between TlN$_3$ and TlHF$_2$ is due to two factors. Firstly, TlN$_3$ is orthorhombic below 233 K, while TlHF$_2$ is tetragonal below this temperature. Secondly, the heat capacity of TlHF$_2$ begins to rise sharply near 300 K possibly as a premonitory effect—similar to that in CsHF$_2$ (compare figure 4)—heralding the onset of a transition in TlHF$_2$ noted in a recent report.[34]

HEAT CAPACITY OF KN₃ FROM SPECTRAL DATA

Heat capacities at constant volume (C_V) of these azides can be calculated from the acoustical and the optical spectral branches. The former contribution can be represented by a Debye term using a characteristic temperature determined from the heat capacity of the solid, and the latter by Einstein terms deduced from the frequencies. The tetragonal azides of this research have two formula units in each primitive cell,[35] 21 optical and 3 acoustical modes. Although spectral data are available for all compounds in this research, only for KN$_3$ and TlN$_3$ are some thermal expansivities and compressibilities available.

For KN$_3$, the C_V calculated from spectral data and that calculated from our measured C_p values with thermal expansivities and compressibilities are displayed in figure 6. As an alternative method for calculating C_V, the familiar relation represented by the first equality:

$$C_p - C_V = TV\alpha^2/\kappa = ATC_p^2,$$

in which V denotes molar volume, α thermal expansivity, and κ isothermal compressibility may be recast as the term shown at the right (in which the symbol A denotes $V\alpha^2/\kappa C_p^2$). A remains approximately constant over significant temperature ranges.[36] For KN_3, a value of A of 1.08×10^{-5} mol cal_{th}^{-1} at 293 K was derived from the molar volume of 39.9 cm^3 mol^{-1}, a temperature-dependent thermal expansivity valid from 100 to 300 K (with a 293 K value of 144×10^{-6} K^{-1},[37] favored over an earlier value of 182×10^{-6} K^{-1},[38]), and a compressibility of 54.1 TPa^{-1}. For TlN_3, the
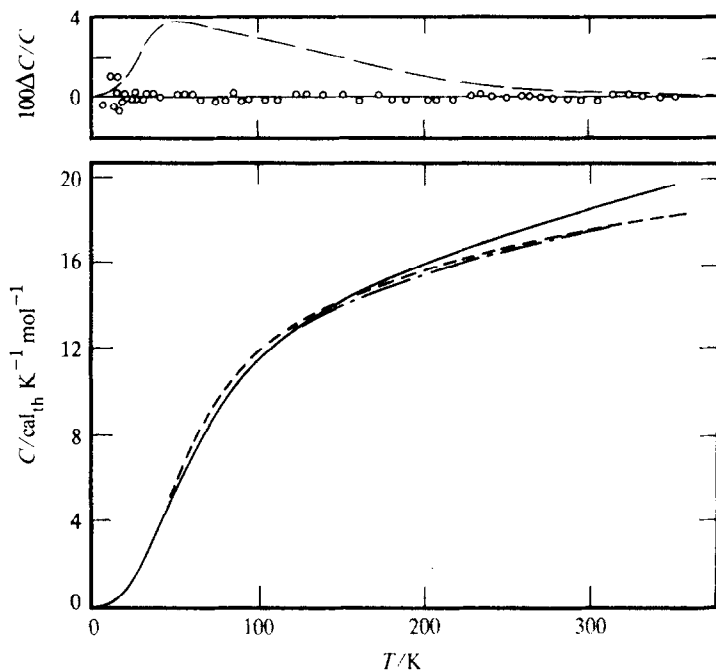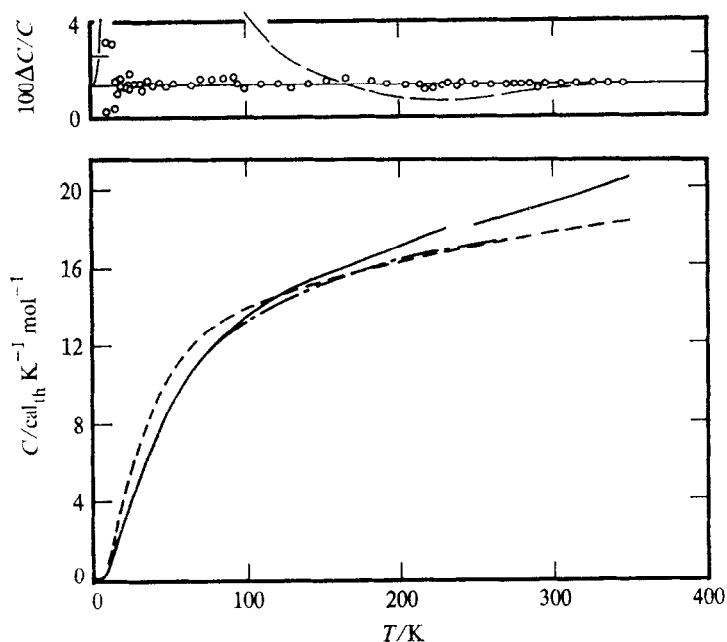

FIGURE 6. Comparison of heat capacity of KN_3 evaluated by different methods. ———, C_p (expt); — — — —, C_V(calc. from spectral data); —··—, C_V(calc. from C_p(expt) adjusted for thermal expansivity and compressibility). The deviations, $\bigcirc$, between the experimental C_p points and the smoothed curve and ——— ——— ——— between the C_V(from spectral data) and C_V(calc. from C_p) are depicted in the upper portion of the figure.

value of A of 1.21×10^{-5} mol cal_{th}^{-1} was deduced from $V = 41.7$ cm^3 mol^{-1}, $\alpha = 135 \times 10^{-6}$ K^{-1} below the TlN_3 transition and 160×10^{-6} K^{-1} above the transition,[12] and $\kappa = 46.3$ TPa^{-1}.[39] Values of C_p(expt) and of C_V(calc.) from the expression above, displayed in figures 6 and 7 show good agreement with C_V(spect.) at high temperatures but deviate as the temperature decreases. Such deviation has been observed in other solids also.[35] Evaluation of C_V from spectral data for NaN_3 and the other two compounds of this study can be found elsewhere;[16] (however, only for KN_3 and TlN_3 are α and κ available). For each of these azides the spectroscopic

FIGURE 7. Comparison of heat capacity of TlN$_3$ evaluated by different methods. ——, C_p(expt); – – – –, C_V(calc. from spectral data); –·–, C_V(calc. from C_p(expt) adjusted for thermal expansivity and compressibility). The deviations, $\bigcirc$, between the experimental C_p points and the smoothed curve and —— —— ——, between the C_V(from spectral data) and C_V(calc. from C_p) are depicted in the upper portion of the figure.

C_V exceeds the measured C_p at lower temperatures. The relative success of the calculation for KN$_3$ probably stems from the greater separation of optical and acoustical branches occasioned by the comparable masses of the two ions.

REFERENCES

1. Part I. Carling, R. W.; Westrum, E. F., Jr., *J. Chem. Thermodynamics* **1976**, 8, 565.
2. Westrum, E. F., Jr.; Burney, G. *J. Phys. Chem.* **1961**, 65, 344.
3. Westrum, E. F., Jr.; Pitzer, K. S. *J. Am. Chem. Soc.* **1949**, 71, 1940.
4. Choi, C. S.; Prince, E. *J. Chem. Phys.* **1976**, 64, 4510.
5. Mueller, H. J.; Joebstl, J. A. *Z. Krist.* **1965**, 121, 385
6. Landee, C. P.; Westrum, E. F., Jr., unpublished results.
7. Evans, B. L.; Yoffe, A. D.; Gray, P. *Chem. Revs.* **1959**, 59, 515.
8. Pistorius, C. W. F. T. *J. Chem. Phys.* **1969**, 51, 2604.
9. Burney, G. A.; Westrum, E. F., Jr. *J. Phys. Chem.* **1961**, 65, 349.
10. Kezer, O. F.; Rosenwasser, H. *Nature* **1966**, 210, 1354.
11. Iqbal, Z.; Malhotra, M. L. *J. Chem. Phys.* **1972**, 57, 2637.

12. Mauer, F. A.; Hubbard, C. R.; Hahn, T. A. *J. Chem. Phys.* **1973,** 59, 3770.
13. Iqbal, Z.; Christoe, C. W. *Chem. Phys. Lett.* **1974,** 29, 623.
14. Pistorius, C. W. F. T. *J. Chem. Phys.* **1974,** 60, 3720.
15. Suhrman, V. R.; Clusius, K. *Z. Anorg. Chem.* **1926,** 152, 52.
16. Carling, R. W., Ph.D. thesis, The University of Michigan, Ann Arbor, Michigan, 1975 *Diss. Abs.* **1976,** 36, 5056–B.
17. For detailed supplementary data concerning X-ray analysis of the samples used in this research, see NAPS document No. 02771 for 12 pages of supplementary material. Order from ASIS/NAPS, c/o Microfiche Publications, 440 Park Avenue South, New York, New York 10016 U.S.A. Remit in advance for each NAPS accession number. Make checks payable to Microfiche Publications. Photocopies are $5.00. Microfiche are $3.00. Outside the U.S. and Canada postage is $2.00 for a photocopy or $1.00 for a fiche.
18. Clem, R. G.; Huffman, E. H. *Anal. Chem.* **1965,** 37, 366.
19. Suzuki, S. *J. Chem. Soc. Jpn., Pure Chem. Sect.* **1952,** 73, 150.
20. Vogel, A. I. *A Text-Book of Inorganic Analysis,* 3rd edition. Wiley: New York. **1961.**
21. Westrum, E. F., Jr.; Furukawa, G. T.; McCullough, J. P. Adiabatic low-temperature calorimetry. In *Experimental Thermodynamics* vol. I. McCullough, J. P.; Scott, D. W.: editors. Butterworths: London. **1968.**
22. Rossini, F. D.; Wagman, D. D.; Evans, W. H.; Levine, S.; Jaffe, I. *Nat. Bur. Stand. Circular No.* **500,** U.S. Government Printing office, Washington, D.C. **1952.**
23. Iqbal, Z. Personal communication. **1975.**
24. Giauque, W. F.; Stout, J. W. *J. Am. Chem. Soc.* **1939,** 58, 1144.
25. White, A. J. C.; Pistorius, C. W. F. T. *J. Chem. Phys.* **1972,** 56, 4318.
26. Iqbal, Z. *Advan. Raman Spec.* **1972,** 1, 188.
27. Clark, J. B. Personal communication. **1976.**
28. Haase, O., unpublished results.
29. Christoe, C. W.; Iqbal, Z. *Solid State Commun.* **1974,** 15, 859.
30. West, C. D. *Z. Krist.* **1936,** 95, 421.
31. Hassel, V. O.; Kringstad, H. *Z. Anorg. Allg. Chem.* **1930,** 191, 36.
32. Hassel, V. O.; Kringstad, H. *Z. Anorg. Allg. Chem.* **1932,** 208, 382.
33. Lee, A. G. *The Chemistry of Thallium.* Elsevier: New York. **1971.**
34. Zil'Berman, B. D.; Fedotova, T. D.; Gabuda, S. P. *Zh. Strukt. Khim.* **1976,** 17, 273.
35. Hathaway, C. E.; Temple, P. A. *Phys. Rev. B* **1971,** 3, 3497.
36. Zemansky, M. W. *Heat and Thermodynamics.* McGraw-Hill: New York. **1957.**
37. Mauer, F. A.; Hahn, T. A. *AIP Conference Proc.* **1971,** 3, 139.
38. Parsons, R. B.; Yoffe, A. D., *Acta Cryst.* **1966,** 20, 36.
39. Weir, C. E.; Block, S.; Piermarini, G. J. *J. Chem. Phys.* **1970,** 53, 4265.